

# The energy spectrum of forward photons measured by the RHICf experiment in $\sqrt{s} = 510$ GeV proton-proton collisions

K. Sato\*,<sup>a</sup> Y. Itow,<sup>a,b</sup> H. Menjo,<sup>a</sup> M. Ueno,<sup>a</sup> K. Ohashi,<sup>a</sup> T. Sako,<sup>c</sup> Y. Goto,<sup>d</sup>  
I. Nakagawa,<sup>d</sup> R. Saidl,<sup>d</sup> J. S. Park,<sup>d,e</sup> M. H. Kim,<sup>d,f</sup> B. Hong,<sup>f</sup> K. Tanida,<sup>g</sup> S. Torii,<sup>h</sup>  
K. Kasahara,<sup>i</sup> N. Sakurai,<sup>j</sup> O. Adriani,<sup>k,l</sup> R. D'Alessandro,<sup>k,l</sup> L. Bonechi,<sup>k</sup> E. Berti,<sup>k</sup>  
and A. Tricomi,<sup>m,n</sup>

<sup>a</sup> Institute for Space-Earth Environmental Research, Nagoya University, Japan

<sup>b</sup> Kobayashi-Maskawa Institute for the Origin of Particles and the Universe, Nagoya University, Nagoya, Japan

<sup>c</sup> Institute for Cosmic Ray Research, the University of Tokyo, Chiba, Japan

<sup>d</sup> RIKEN Nishina Center for Accelerator-Based Science, Saitama, Japan

<sup>e</sup> Seoul National University, Seoul, South Korea

<sup>f</sup> Korea University, Seoul, South Korea

<sup>g</sup> Japan Atomic Energy Agency, Ibaraki, Japan

<sup>h</sup> Waseda University, Shinjuku, Tokyo, Japan

<sup>i</sup> Shibaura Institute of Technology, Tokyo, Japan

<sup>j</sup> Tokushima University, Tokushima, Japan

<sup>k</sup> INFN Section of Florence, Florence, Italy

<sup>l</sup> University of Florence, Florence, Italy

<sup>m</sup> INFN Section of Catania, Catania, Italy

<sup>n</sup> University of Catania, Catania, Italy

E-mail: sato.kenta@isee.nagoya-u.ac.jp

The Relativistic Heavy Ion Collider forward (RHICf) experiment aims at understanding the high-energy hadronic interaction by measuring the cross sections of very forward neutral particles in proton-proton collisions at  $\sqrt{s} = 510$  GeV. For the analysis of the photon measurement, the trigger efficiency and the particle identification performance are studied by using the Monte Carlo simulation data and the experimental data. In the RHICf operation, two kinds of trigger modes (Shower, HighEM) were implemented. The trigger efficiency of the Shower trigger is 100% for photons with the energies more than 20 GeV. The HighEM trigger is designed to detect high energy photons effectively, and the trigger efficiency of the HighEM trigger is 90% for photons with the energies more than 130 GeV. The correction factor for the photon identification is calculated by using the efficiency and purity. It is found that this correction does not make a sizeable effect on the shape of the energy spectrum because the energy dependency of the factor is small.

36th International Cosmic Ray Conference -ICRC2019-  
July 24th - August 1st, 2019  
Madison, WI, U.S.A.

\*Speaker.

## 1. Introduction

The origin of cosmic rays is not known well. The mass composition of cosmic rays is a very important observable in order to understand the cosmic ray sources [1]. Very high energy cosmic rays with the energies more than  $10^{15}$  eV are observed by using the extensive air shower technique [2]. For interpretation of the mass composition of cosmic rays from an observable, such as the depth of shower maximum, the air-shower Monte Carlo (MC) simulation is a mandatory tool. However, it is difficult because of the uncertainties of the hadronic interaction models used in the simulation [3]. These interaction models must be tested and tuned by using the experimental data obtained under well-controlled conditions as collider experiments. Large Hadron Collider (LHC) provided many experimental data measured in  $pp$  collisions with several collision energies. One of the LHC experiments, LHCf, measured the production cross-section of energetic photons emitted into the very forward region of collisions [4, 5, 6]. For air-shower development induced by high-energy cosmic-rays, the production cross-section of photons is very important, and it should be measured at several collision energies in order to understand the collision-energy dependency of it. The LHCf published the results of their photon measurements at three collision energies in centre-of-mass frame,  $\sqrt{s} = 0.9, 7$  and  $13$  TeV, however, the transverse momentum coverage of the measurement at the lowest energy,  $p_T < 0.12$  GeV, is too small to study the collision-energy dependence of the forward photon production.

We brought one of the LHCf detectors, called Arm1 [7], to the Relativistic Heavy Ion Collider (RHIC) at the Brookhaven National Laboratory in USA. The RHIC forward (RHICf) experiment enables to measure forward photons in  $pp$  collisions at  $\sqrt{s} = 510$  GeV with the same  $p_T$  coverage as in the LHCf  $\sqrt{s} = 7$  TeV measurement because the RHICf detector is installed at 18 m from the interaction point, which is much closer than at the LHCf measurement (140 m). Comparing the RHICf data with the LHCf data, the collision-energy dependency of forward particle production can be measured, which is essential to precisely interpolate and extrapolate the experimental results from  $10^{14}$  eV to  $10^{17}$  eV and above in the laboratory frame.

In this paper, we present the trigger efficiency and the particle identification performance of the RHICf experiment, which are important for the measurement of the photon energy spectrum. In Section 3, the trigger efficiency is calculated by using the MC simulation data after introducing about the trigger modes of the RHICf experiment. In Section 4, the correction factor about the photon identification is reported, then the contribution to the energy spectrum is discussed.

## 2. The RHICf experiment

The RHICf aims to understand the hadronic interaction by measuring the differential production cross-sections of very forward particles at RHIC. The RHICf operation was successfully completed with  $pp$  collisions at  $\sqrt{s} = 510$  GeV in June, 2017 [8]. The RHICf detector consists of two sampling calorimeters (Fig.1), and it detects neutral particles such as photons, neutrons, and neutral pions. It was installed at 18 m to the west of the interaction point where the STAR detector locates. The dimensions of their calorimeters are  $20 \text{ mm} \times 20 \text{ mm}$  and  $40 \text{ mm} \times 40 \text{ mm}$ . The RHICf detector covers the pseudorapidity range  $\eta > 6$ . Each calorimeter is composed of tungsten plates, 16 GSO scintillator layers for shower sampling, and 4 X-Y GSO bar hodoscopes for impact

position determination of showers. The longitudinal size of the calorimeters is 44 radiation lengths and 1.6 hadronic interaction lengths. The energy and position resolutions for 200 GeV photons are 5% and 200  $\mu\text{m}$ , respectively [7]. The RHICf measurement was performed at the three different positions (Bottom, Middle, Top). In the Middle position, the centre of the small calorimeter was located at the projection point of the beam axis at the interaction point to the RHICf detector location. The Bottom and Top positions are shifted vertically from the Middle position at -47.4 mm and 24.0 mm, respectively. The total operation time with collisions in the 2017 operation was approximately 28 hours.

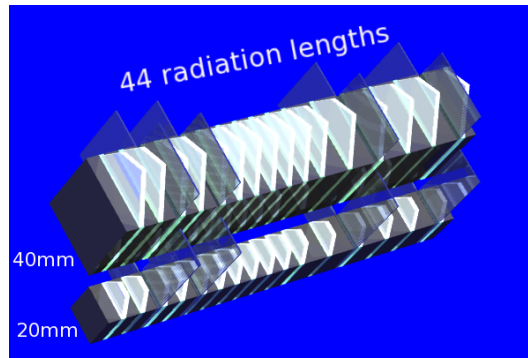


**Figure 1:** The schematic view of the RHICf detector

### 3. The Trigger efficiency

Three trigger modes (Shower,  $\pi^0$ , and HighEM) are implemented in the RHICf trigger system [8]. The Shower trigger mode is designed for detecting photons and neutrons, and the  $\pi^0$ , and HighEM are for detection of relatively rare events of  $\pi^0$ , and high energy photon effectively. Each trigger mode issues a trigger signal by using the information of the sampling layers. The Shower trigger mode detects any electromagnetic and hadronic showers induced by photons and neutrons. The trigger signal is issued when the energy deposit in any three successive layers are more than 45 MeV. The  $\pi^0$  trigger mode detects photon pairs from  $\pi^0$  decays. The trigger signal is issued when a electromagnetic shower is simultaneously induced in each tower. These Shower and  $\pi^0$  trigger modes are originally designed for the LHCf experiment. In addition to them, the HighEM trigger mode is newly designed to detect only energetic photons with the energies of more than 100 GeV. The trigger signal is issued when the energy deposit in the fourth layer is more than 500 MeV. Final trigger signals are issued after mixing these three kinds of trigger signals. The trigger rate of each trigger mode was independently optimised by applying prescale before the trigger mixing. The typical prescale factors are 20, 1, 2 for the Shower,  $\pi^0$ , and HighEM, respectively. These factors were continuously optimised during the RHICf operation to cope with the limited data acquisition speed.

The RHICf trigger efficiency is estimated on the basis of a MC simulation using Geant4. In this study, hardware behaviours such as the discriminator response and the pedestal fluctuation in each layer obtained from the experimental data are considered. The efficiency of the Shower

triggers is 100% for photons with the energy more than 20 GeV (Fig. 2 (left)). The efficiency of the HighEM triggers is 90% for high-energy photons with the energies more than 130 GeV (Fig. 2 (right)). Figure 3 shows  $\Sigma dE$  spectra of photon events obtained during a 30 min. RHICf run, where

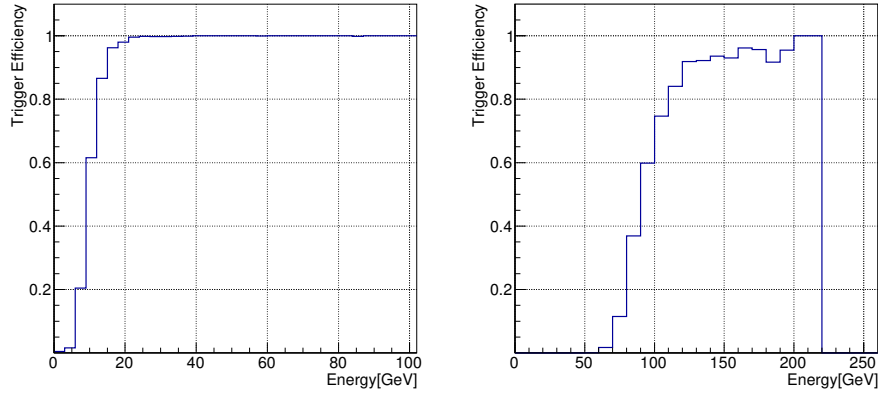


**Figure 2:** The trigger efficiency in the function of the incident photon energy. (left) Shower trigger mode (right) HighEM trigger mode

$\Sigma dE$  is defined as the summation of the deposited energies from the second layer to the thirteenth one. The event selection discussed in the next section is applied. The maximum  $\Sigma dE$  reaching at 9 GeV corresponds to the incident photon energy of approximately 250 GeV, which is equivalent to the beam energy. The blue and red curves indicate the number of events recorded by the Shower and HighEM triggers, respectively. The total numbers of the Shower events and of the HighEM events with  $\Sigma dE > 4.5$  GeV are  $1.7 \times 10^3$  and  $1.3 \times 10^4$ , respectively. Considering the total operation time of 11 hours in the Middle position run, the total numbers of events obtained at the detector position reach  $3.7 \times 10^4$  and  $2.9 \times 10^5$  in the Shower and HighEM samples, respectively. Thanks to the HighEM trigger mode, the high energy photon data are effectively obtained, and the total number of the recorded HighEM events is 7.9 times larger than that of Shower events with  $\Sigma dE > 4.5$  GeV. Suppose the HighEM trigger is not implemented, which corresponds to an operation with no prescaling of each trigger signals, the Shower trigger rate in the RHICf-Run2798 was increased by a factor 1.86. Even considering the factor, the total number of detected high-energy photon events was increased by a factor of  $7.9 / 1.86 = 4.2$ .

#### 4. Photon Identification performance

The energy spectra are measured through the processes on the event reconstruction, event selections, and corrections. In this analysis, we follow the analysis method used in the measurement of the LHCf experiment [6]. The energy, position and particle type (PID) of an incident particle are reconstructed by using the energy deposit in each sampling layer and position sensitive layer. In this photon analysis, single hit photons, defined as photons entering in either the small or large calorimeters without any other particle hitting the detector, are used. Here, the photon, which does not enter in a certain fiducial area of the detector, is rejected. The photon identification uses the

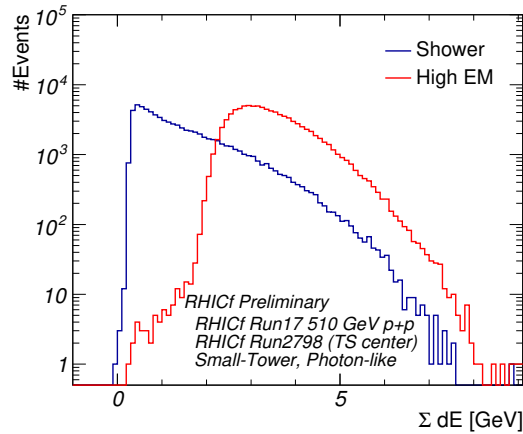


**Figure 3:** The number of photons obtained in the RHICf-Run2798. The blue and red lines show the Shower trigger events and the HighEM trigger events, respectively.

information obtained in the reconstruction process, however, there are leak-out photon events and leak-in neutron events when a certain criterion is applied. The amounts of these inefficiency and contamination must be understood by using the experimental data and the MC simulation data. Incident photons and neutrons induce electromagnetic showers and hadronic showers, respectively. A characteristic property of the photon events is that electromagnetic showers develop in the shallow part of the calorimeter. A PID estimator  $L_{90\%}$  is introduced here, which is defined as the longitudinal depth in the unit of radiation length, where the energy deposit integrated from the first layer reaches 90% of the total measured energy deposit in the calorimeter. Figure 4 shows the fractional accumulated energy deposits of a typical photon (black) and a typical neutron (red) initiated showers. The  $L_{90\%}$  values for the photon and neutron events are indicated as the black and red arrows, respectively. Figure 5 shows the distribution of  $L_{90\%}$  values measured by the RHICf small calorimeter. The red, blue, and green histograms show the distributions of MC simulation data for the photon, neutron, and all (photon + neutron) events, respectively. They are normalized with factors obtained from a fitting discussed below. A reasonable cut threshold is expected to be around 15-20, where the dominant component transits from photons to neutrons.

In this analysis, the simulation data of the proton-proton collisions using the QGSJETII-04 [9] generator together with the detector response calculation using the Geant4 package are used. It contains  $3.0 \times 10^7$  inelastic collision events, which corresponds to a statistics of a 30 minutes operation data in the RHICf experiment. The cut threshold of  $L_{90\%}$  in each photon energy region is optimised as the detection efficiency  $\varepsilon$  reaches at 90% (Fig. 6 (left)). Increasing the photon energy, the cut threshold varies from 13.5 to 17.0 as shown in Fig 6 (right). The red line shows the fitting result by a logarithmic-function in the region between 30 GeV and 130 GeV. In the energy region of more than 130 GeV, the threshold value is extrapolated by using this fitting function. The purity  $p$ , which indicates the fraction of true photon events over all selected events, is introduced here. The purity  $p$  is calculated by using the template fitting method. The experimental data is fit by using the  $L_{90\%}$  template distributions obtained from true photon and neutron simulation events. The normalization factors of these template distributions are free parameters in this fitting. Figure 7 (left)

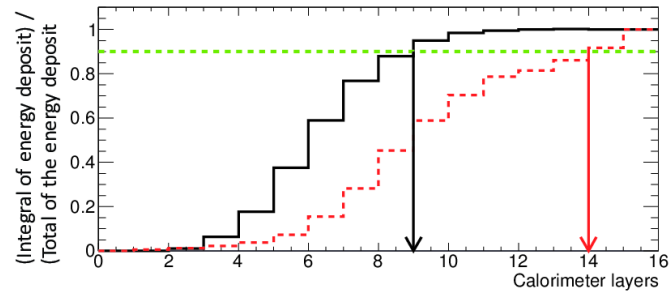


**Figure 4:** The ratio of the measured energy-deposit integrated from the first layer to the total measured energy-deposit in each layer for typical photon (black solid) and neutron (red dotted) events. Horizontal axis shows the longitudinal depth in the unit of radiation length. The black and red arrows indicate the  $L_{90\%}$  values in the photon and neutron events, respectively.

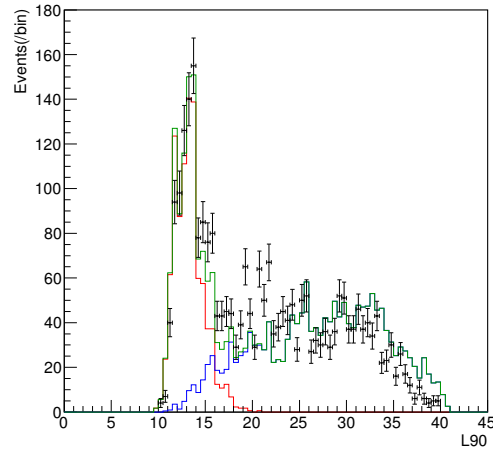


**Figure 5:** The  $L_{90\%}$  distribution measured by the small calorimeter. Only the events with the reconstructed energy between 70 GeV and 80 GeV are used. The red and blue histograms show the MC distribution of the photon events one and the neutron events, respectively. The green line shows all (photon + neutron) events.

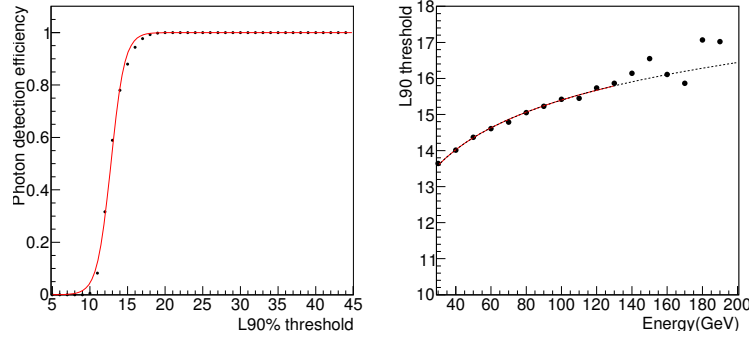


**Figure 6:** (left) The identification efficiency by using  $L_{90\%}$  cut parameter. The red line shows the adhoc function to interpolate the point the detection efficiency reaches 90%. (right) The energy dependence of the  $L_{90\%}$  cut parameter. The red line is the fitting logarithmic-function.

shows the purity  $p$  and the efficiency  $\varepsilon$  as a function of the photon energy, which are calculated from the fitting results. In this analysis, the experimental data, which contains  $7.0 \times 10^5$  Shower trigger events, is used.

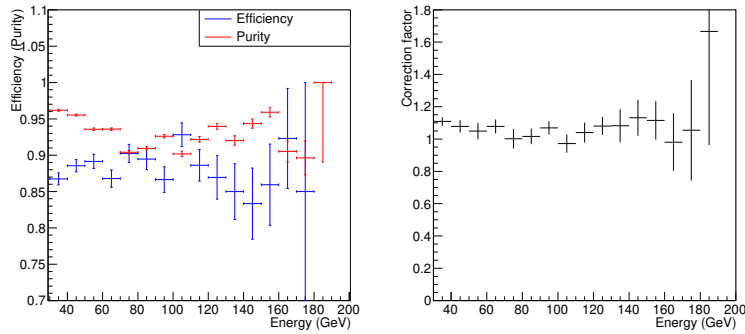


**Figure 7:** (left) Photon identification performance. The blue and red points show the identification efficiency  $\varepsilon$  and purity  $p$  as a function of the photon energy. The error of the efficiency  $\varepsilon$  shows the statistical uncertainty and the error of the purity  $p$  shows the statistical uncertainty and the uncertainty propagated from the template fitting. (right) The correction factor  $p/\varepsilon$  for the photon identification process. The error bar shows the uncertainty calculated by considering the propagation from the purity and efficiency.

The correction factor for the particle identification is calculated as  $p/\varepsilon$ . Figure 7 (right) shows the correction factor as a function of the photon incident energy. The factor shows a small energy dependence.

## 5. Summary

The RHICf experiment aims at understanding the hadronic interaction by measuring the cross sections of very forward neutral particles in proton-proton collisions at  $\sqrt{s} = 510$  GeV. The operation was completed successfully in 2017. In the RHICf trigger system, three trigger modes are

implemented due to obtain the high-energy photon events effectively. The efficiency of the Shower trigger and the HighEM trigger are 100% for photons with the energies more than 20 GeV and 90% for high-energy photons with the energies more than 130 GeV, respectively. The total number of detected high-energy photon events was increased by a factor of 4.2.

In the RHICf analysis, the photon events are identified by using the  $L_{90\%}$  parameter. The PID performances, purity and efficiency, are estimated from the template fitting method using distributions for photons and neutrons obtained from the simulation sample. The correction factor for the identification process is calculated by using the purity  $p$  and the efficiency  $\varepsilon$ . The correction factor  $p/\varepsilon$  shows a small energy dependency.

## Acknowledgment

The RHICf collaboration is grateful to the people related to the RHIC, the STAR collaboration, the PHENIX collaboration and the LHCf collaboration to support the experiment. This program is partly supported by the Japan-US Science and Technology Cooperation Program in High Energy Physics. A part of this work was performed using the computer resource provided by the Institute for the Cosmic-Ray Research (ICRR), University of Tokyo.

## References

- [1] V. Berezhinsky, A.Z. Gazizov, S.I. Grigorieva, *Dip in UHECR spectrum as signature of proton interaction with CMB*, *Phys Lett.* **612**, (2005) 147-153.
- [2] Pierre Auger Collaboration, *The Pierre Auger Cosmic Ray Observatory*, *Nuclear Instruments and Methods in Physics Research A* **798**, (2015) 172-213.
- [3] The Pierre Auger Collaboration, *Muons in air showers at the Pierre Auger Observatory: Measurement of atmospheric production depth*, *Phys. Rev. Lett.*, **90**, (2014) 012012
- [4] O. Adriani. et al., *Measurement of zero degree inclusive photon energy spectra for  $\sqrt{s}=900$  GeV proton-proton collisions at LHC*, *Physics Letters B* **715** (2012) 298-303
- [5] O. Adriani. et al., *Measurement of zero degree single photon energy spectra for  $\sqrt{s}=7$  TeV proton-proton collisions at LHC*, *Physics Letters B* **703** (2011) 128-134
- [6] O. Adriani. et al., *Measurement of forward photon production cross-section in proton-proton collisions at  $\sqrt{s}=13$  TeV with the LHCf detector*, *Physics Letters B* **703** (2018) 233-239
- [7] LHCf Collaboration, *The LHCf detector at the CERN Large Hadron Collider*, *JINST* **3**, S08006 (2008).
- [8] H. Menjo et al., *DAQ performances of the RHICf operation in 2017*, *RIKEN Accel. Prog. Rep.* **51** (2018) 115.
- [9] S. Ostapchenko., *Monte Carlo treatment of hadronic interactions in enhanced Pomeron scheme: QGSJET-II model*, *Phys. Rev.* **D 83**, (2011), 014018.